Title

cyclic-di-GMP drives innate lymphoid cells changes through the STING-cGas pathway during type-2 lung inflammation

Author

Lacasa, Lee Diego Lace

Publication Date

2021

Peer reviewed|Thesis/dissertation

UNIVERSITY OF CALIFORNIA SAN DIEGO

cyclic-di-GMP drives innate lymphoid cells changes through the STING-cGas pathway during type-2 lung inflammation

A thesis submitted in partial satisfaction of the requirements
for the degree Master of Science

in

Biology

by

Lee Diego Lace Lacasa

Committee in charge:

Professor Taylor Doherty, Chair
Professor Alistair Russell, Co-Chair
Professor Katherine Petrie

2021

The Thesis of Lee Diego Lace Lacasa is approved, and it is acceptable in quality and form for publication on microfilm and electronically.

University of California San Diego

2021

DEDICATION

This work is dedicated to my bayanihan, my community, my roots. To my family and ancestral line, for their countless sacrifices and steadfast faith in my dreams, for which I navigate each opportunity with immense gratitude and unfailing perseverance. And to extended loved ones, for their immense love and support, for I am grateful to know and receive love, and understand the value of community. *To exceed the limit of limits* – A.E.P.

EPIGRAPH

Although the way ahead [for immunology] is full of pitfalls and difficulties, this is indeed an exhilarating prospect. There is no danger of a shortage of forthcoming excitement in the subject. Yet, as always, the highlights of tomorrow are the unpredictabilities of today.

César Milstein

TABLE OF CONTENTS

LIST OF FIGURES

ACKNOWLEDGEMENTS

First and foremost, I would like to acknowledge Dr. Taylor Doherty for his invaluable support and guidance. Dr. Doherty's commitment to my growth afforded me a repertoire of skills and knowledge base I would not have cultivated elsewhere. His expertise, enthusiasm, and counsel were instrumental towards the completion of this project and my training.

Secondly, I would like to acknowledge all my former research mentors who invested in my yearning in scientific inquiry, for I would not have reached this milestone without prior dedicated guidance and genuine care. Finally, I would like to acknowledge past and present members of the Doherty lab, especially Allyssa Strohm, Anthea Leng, Yung-an Huang, and Jana Badrani, for their support and camaraderie, allowing me to grow in a space dedicated to scientific inquiry and collaboration.

The content of this thesis is a reprint of the material as it appears in Cyclic-di-GMP Induces STING-Dependent ILC2 to ILC1 Shift During Innate Type 2 Lung Inflammation 2021. Cavagnero, Kellen; Badrani, Jana; Naji, Luay; Amadeo, Michael; Leng, Anthea; Lacasa, Lee Diego; Strohm, Allyssa; Renusch, Samantha; Gasparian, Suzanna; Doherty, Taylor, Frontiers Media S.A., 2021. The thesis author was a co-author of this paper.

ABSTRACT OF THE THESIS

cyclic-di-GMP drives innate lymphoid cells changes through the
STING-cGas pathway during type-2 lung inflammation

by

Lee Diego Lace Lacasa
Master of Science in Biology

University of California San Diego, 2021

Professor Taylor Doherty, Chair
Professor Alistair Russell, Co-Chair

Type 2 inflammation plays a critical role in most asthmatic cases and may be affected during recurring viral and bacterial infections. The presence of intracellular pathogens promotes the buildup of danger signaling cyclic-di-nucleotide molecules such as cyclic-di-GMP (CDG), a bacterial second messenger. Group 2 innate lymphoid cells (ILC2s) are major contributors to type 2 inflammatory responses after exposure to fungal allergens yet the role of CDG in regulating pulmonary ILC responses in inflammation remains to be seen. Our studies demonstrate that intranasal exposure to CDG drives early type 1 interferon (IFN) production and effectively suppresses type 2 lung inflammation and CD127+ST2+ ILC2s during *Alternaria* challenge in a

STING-cGAS dependent manner. Interestingly, CDG drove activation and expansion of ST2-CD127- pulmonary ILCs, which exhibit a transcriptomic profile consistent with ILC1s. Overall, CDG has demonstrated a suppressive effect on type 2 inflammatory responses while simultaneously promoting ILC1 activation. Our findings suggest that there is potential to utilize STING to mediate type 2 inflammatory responses and/or promote anti-viral immunological mechanisms.

INTRODUCTION

Asthma is one of the leading chronic non-communicable diseases worldwide, affecting roughly 334 million people [1] and driving increases in morbidity rates and health care expenditure [2]. Though effective interventions exist to alleviate asthma symptoms, asthma continues to cause substantial disability, compromised quality of life, and avoidable deaths in children to young adults [1]. Asthma as a heterogenous condition arises from various underlying mechanisms (endotype) that drive an array of observable disease characteristics (phenotype) [1]. The disease phenotypes reflect vast complex host-environment interactions that occur over spatial (i.e., genetic to cellular to tissue to organ) and time scales [1]. However, the main pathological hallmarks include airway hyperresponsiveness (AHR), bronchial muscle constriction, excessive mucus production, and airway remodeling, as a collection of immune responses to environmental inhalants damaging the airway epithelium [3]. Airway epithelial damage causes the release of signaling molecules called "alarmins" to promote the recruitment of granulocytes, a group of immune cells containing enzymatic granules that are released into the local environment during infections [4]. Granulocytes are the main cellular infiltrates during inflammatory responses, usually recruited by cytokine signaling from tissue-resident cells [4].

Eosinophilic, type 2 airway inflammation is conventionally classified by the activation of adaptive T helper 2 (Th2) cells following allergic sensitization and consequent stimulation by tissue-resident dendritic cells near the airway epithelium [1]. Upon activation, Th2 cells promote cell-mediated responses mainly through the production of the obligate IL-5 cytokine for eosinophil recruitment, IL-4 to promote IgE synthesis to activate mast cells and IL-13 for increased mucus production and AHR [1]. In contrast, non-allergic eosinophilic asthma is mediated by the innate immune response, demonstrating an early time point of IL-5 and IL-13 secretion following

epithelium released alarmins IL-25 and IL-33 after epithelial damage by microbes and pollutants [1]. The differing allergic-dependent (IgE-mediated, adaptive immunity) and -independent (innate immunity) mechanisms that underly eosinophilic asthma can co-occur, driving mixed granulocytic inflammation or adaptations in the host inflammatory profile over time. While Th2 cells mediate allergic-dependent asthma, a specific innate cell type mediates the allergic-independent response.

Among the many immune cells modulating the response to infection, innate lymphoid cells (ILCs) are tissue-resident cells that orchestrate the first line of pathogenic defense and function similarly to CD4+ T helper (Th) cells. ILCs are non-circulatory tissue-resident cells and are revered to be the innate counterparts of CD4+ T-helper (Th) cells [6]. While Th cells are adaptive immune cells well classified by their cell surface receptors, ILCs lack lineage specifying markers [6]. However, ILCs and Th cells share common cellular progenitors, phenotypic, transcriptional, and functional characteristics [7, 8]. The subsets of ILCs, namely ILC1, ILC2, and ILC3, parallel Th1, Th2, and Th17/22 cells, respectively through their characteristic expression of transcription factors and effector cytokine production [6].

Group 2 innate lymphoid cells (ILC2s) contribute to innate type 2 lung inflammation through secretion of type 2 cytokines that promote the hallmarks of asthma [8]. Indeed, this consequently centerpieces ILC2s as the main contributor during the onset of non-allergic eosinophilic inflammation [9]. Damage to airway epithelium leads to the release of TSLP, IL-25, and IL-33 which induce ILC2 activation to produce type 2 cytokine secretion [10]. Additionally, ILC2s can initiate and amplify the innate responses and facilitate the onset of adaptive immunity over time [10]. However, our understanding of complex mechanisms that mediate diverse pathogen infections that lead to asthma remains to be seen.

While type 2 inflammation is a major contributor to the development of asthma, it may co-occur with intracellular viral infections and bacterial colonization. The STING-cGAS pathway, comprised of the "stimulator of interferon genes" (STING) and synthase for the second messenger cyclic GMP-AMP (cGAS), is an innate cellular intrinsic signaling mechanism mainly implicated in intracellular pathogenic infections [11]. When cGAS binds to non-self-DNA, it concurrently converts ATP and GTP into a cyclic-di-nucleotide, which can then trigger activation of ER-bound STING [12, 13]. Ultimately, the STING-cGAS activation elicits transcription of a family of signalling molecules, type-1 interferons (IFNs) [14]. Interferons are known to play a major role in pathogen clearance and inflammation, and thus are the major response to the detection of pathogenic DNA. In asthma, STING activation with cyclic-di-nucleotide molecules has shown to contribute to the progression of non-eosinophilic, type 1 inflammation.

A recent study by Raundhal et al. 2015 looked at the resulting cytokines after intranasal challenge of house dust mite (HDM) and cyclic-di-GMP (CDG) in a 28-day model [15]. Raundhal et al. 2015 revealed that CDG promoted neutrophilia in an HDM model, and HDM drove suppression of eosinophilic inflammation [15]. Our group aimed to elucidate related mechanisms of innate immunity through airway exposure of clinically relevant fungal allergen *Alternaria alternata* (Alt) and CDG using wild-type*, Tmem173-/- (sting-/-),* and *ifnαr1-/-* mice. Alt is known to potently promote epithelial IL-33 secretion, upstream of ILC2 production of IL-5 and IL-13, driving eosinophilic inflammation [16], whereas CDG has previously demonstrated suppressive effects on type 2 inflammation. Thus, it is suspected that airway exposure of Alt and CDG will negatively regulate innate type 2 inflammation in a STING-dependent manner. Comparison of each background strain and their resulting immunological responses to Alt and CDG challenge can

help determine specific mechanistic details of suppressing type 2 inflammation through STING-cGAS signaling.

MATERIALS AND METHODS

Mice

6- to 12-week-old female C57BL/6 WT mice were acquired from The Jackson Laboratory (Bar Harbor, Me). *Ifnar1*-/- and *Tmem173*-/- mice were acquired from The Jackson Laboratory and bred in-house. Red5 mice were acquired from Dr. Nunzio Bottini (UCSD), originating from Dr. Richard Locksley (UCSF), and bred in-house [17]. Smart13 mice were acquired from The Jackson Laboratory, originating from Dr. Richard Locksley (UCSF), and bred in-house [18]. All animal experiments were approved by the University of California, San Diego Institutional Animal Care and Use Committee.

In vivo Alternaria and CDG model

WT, gene knockout, and cytokine reporter mice were challenged intranasally with PBS, 5 µg CDG, 50 µg of *Alt* extract (Greer, lot number 299382), or 5 µg CDG and 50 µg *Alt* extract in 40 µL every 24 h over 3 days, then euthanized 24 h following the third challenge for BAL supernatant collection and lung tissue harvest. A subset of experiments was completed with only the latter two experimental groups. For experiments in which ILCs were isolated, mice were challenged with *Alt* four times over 10 days for expansion of ILC population. For experiments investigating early cytokine release, mice were euthanized 3 h following one challenge. BAL was performed with 2% BSA in PBS; the first draw was 500 µL and subsequent draws 2 through 5 were 600 µL. BAL was centrifuged at 1,500 rpm for 5 min at 4°C and the supernatant was stored at −20°C for ELISA. BAL cells were counted and phenotyped using flow cytometry. Lungs were digested using the Mouse Lung Dissociation Kit (Miltenyi Biotec) following the manufacturer's

protocol, filtered with a 40 μm mesh, and cells were counted and phenotyped using flow cytometry.

Flow Cytometry

BAL and lung cells were resuspended in a solution of 0.01% sodium azide and 2% FBS in PBS then counted on a Novocyte (Acea Biosciences). One million BAL cells were aliquoted into tubes then incubated with an unconjugated monocloncal antibody (mAb) to CD16/CD32 for 10 min at 4°C to block non-specific Fc receptor binding, and then incubated for 30 min with fluorochrome conjugated antibodies at 4°C. All antibodies were purchased from BioLegend unless otherwise noted. To identify eosinophils (CD45+ CD11c- Siglec-F+) and neutrophils (CD45+ Siglec-F- GR-1+), BAL or lung cells were stained with PerCP-conjugated anti-CD45.2, PE-conjugated anti-Siglec-F (BD), FITC-conjugated anti-CD11c, and APC-conjugated anti-GR-1. For the identification of ILCs (CD45.2+lineage-Thy1.2+ lymphocytes), ILC2s (CD45.2+lineage-Thy1.2+CD127+ST2+), and ILC1s (CD45.2+lineage-Thy1.2+CD127-ST2-) lung cells were incubated with FITC–conjugated lineage cocktail (anti-B220, anti-CD11b, anti-CD3e, anti-GR-1, anti-Ter119), anti-CD5, anti-CD11c, anti-FcεR1, anti-NK1.1, anti-TCRβ, and anti-TCRγδ; PerCP-conjugated anti-CD45.2; eFluor 450-conjugated anti-Thy1.2 (ThermoFisher); PE-Cy7-conjugated anti-CD127; and APC-conjugated anti-ST2. In select experiments, ILCs were also stained with PE-conjugated anti-CD69. For the identification of NK cells (CD3-CD49b+NK1.1+), lung cells were incubated with APC-conjugated anti-CD3, PerCP-conjugated anti-CD45.2, PE-conjugated anti-CD49b, and FITC-conjugated anti-NK1.1.

For identification of transcription factor, surface-stained cells were fixed and permeabilized with an intracellular staining kit (ThermoFisher) following the manufacturer's

protocol and stained for 30 min at 4°C with PE-conjugated anti-GATA-3 (ThermoFisher), anti-Ki67 (ThermoFisher), or anti-T-Bet.

For ILC and NK cytokine staining, lung cells from WT and gene knockout mice were incubated at 37°C for 3 hr with a phorbol 12-myristate 13-acetate, brefeldin A, ionomycin, ,nd monensin cell stimulation cocktail (ThermoFisher) in RPMI 1640 media enriched with 10% FBS, 2-mercaptoethanol, glutamine, and penicillin/streptomycin (ThermoFisher). Cells were harvested after culture and surfaced stained for ILC2s and ILC1s as described above, fixed and permeabilized with an intracellular cytokine staining kit (BD) following the manufacturer's protocol, and stained for 30 min at 4°C with PE-conjugated anti-IL-5 or anti-IL-13 and APC-Cy7-conjugated anti-IFNγ.

To assess cytokine staining *ex vivo* without stimulation, reporter mice described previously were used. To visualize *in vivo* IL-5 in Red5 mice, Red5 staining occupied the PE channel without any requisite staining [17]. To visualize *in vivo* IL-13 in Smart13 mice, Smart13/human CD4 was stained with PE-conjugated anti-human CD4 [18]. DAPI (ThermoFisher) staining was used to discriminate live and dead cells. Lastly, samples were analyzed with a Novocyte (Acea Biosciences) flow cytometer or sorted with a FACSAria II (BD) at the UCSD Human Embryonic Stem Cell Core Facility.

In vitro stimulation

Sorted ILCs rested *in vitro* for 48 h with 10 ng/ml IL-2 and IL-7. Media replacement followed the 48 h resting period, and ILCs were subsequently cultured with the following conditions: IL-2 (10 ng/ml) and IL-7 (10 ng/ml); IL-2 (10 ng/ml), IL-7 (10 ng/ml), CDG (10 μM); IL-2 (10 ng/ml), IL-7 (10 ng/ml), and IL-33 (30 ng/ml); or IL-2 (10 ng/ml), IL-7 (10 ng/ml), IL-

33 (30 ng/ml), and CDG (10μM). Cell culture supernatants were collected for ELISA after 24 h of *in vitro* stimulation.

ELISA

ELISAs for IFNβ (R&D), IFNγ (ThermoFisher), IL-5 (R&D), and IL-13 (R&D), were conducted on BAL supernatants following the manufacturers' protocols. ELISAs were read on a model 680 microplate reader (Bio-Rad) at 450 nm.

RNAseq

Publicly available RNA sequencing of mouse lung ILC2s and ILC1s (GEO: GSE136156) was downloaded and analyzed. Reads were aligned to reference genome mm10 using TopHat. DUST scores were incorporated with PRINSEQ Lite, while low complexity reads (DUST > 4) were removed from the BAM files. Read counts for each genomic feature were acquired with the HTSeq count program. Differentially expressed genes were identified using DESeq2 and pathway analysis was conducted via Metascape.

Data and Statistical Analysis

Flow cytometry data were analyzed using FlowJo (Flowjo). For all experiments (except RNAseq), GraphPad Prism software (GraphPad) was used for statistical analysis, using unpaired *t*-tests (2-tailed). *P*-values of < 0.05 were considered statistically significant.

RESULTS

CDG suppresses ILC2-driven type 2 inflammation and promotes interferon secretion

To determine whether CDG regulates innate respiratory immunity, we followed a validated 3-day *Alt*-induced ILC2-driven model of eosinophilic inflammation (**Figure 1**) [16]. Intranasal CDG treatment nearly eradicated *Alt*-induced eosinophilia in bronchoalveolar lavage (BAL) fluid and lungs (**Figure 2A, B**). Additionally, CDG treatment significantly attenuated BAL IL-5 and IL-13 levels (**Figure 3A**). Strikingly, CDG synergistically enhanced *Alt*-induced BAL and lung neutrophilia (**Figure 2A, B**).

Current understanding of interferon interactions with ILC2 driven type 2 cytokine production points towards global suppressive impacts [19-21]. Thus, we aimed to determine whether CDG promoted IFN production during *Alt* treatment. Certainly, BAL IFNγ (type 2 IFN) production increased over 20-fold on average after *Alt* plus CDG treatment relative to *Alt* treatment alone (**Figure 3A**). Further, BAL IFNß (type 1 IFN) production increased 30-fold in CDG challenged mice 3 h post-challenge (**Figure 3B**). Collectively, the results thus far demonstrate that *Alt* plus CDG treatment induces a neutrophil-dominant response associated with higher type 1 and 2 IFN production. Additionally, the results suggest that CDG attenuates innate eosinophilic respiratory inflammation.

CDG promotes an immunological shift in pulmonary ILC2s to ILC1s

Following airway infiltrate immunophenotyping, we next aimed to elucidate the effect of CDG on ILC2 activity in the 3-day *Alt* model. With the observable increases in BAL type 2 IFNs, we additionally aimed to investigate ILC1 responses post CDG exposure. ILC subsets exhibit heterogeneity and plasticity under ranging conditions [16, 22]. Therefore, prior to investigating the

effect of *in vivo* CDG challenge on ILCs, we utilized transcriptomic analysis to validate ILC1s and ILC2s identities following *Alt* treatment. We reanalyzed our existing RNAseq dataset of *Alt* challenged CD127+ST2+ and CD127-ST2- ILCs (**Figure 4**) [16] and found that CD127+ST2+ ILCs highly expressed ILC2-specific genes (Areg, Gata3, Il1rl1, Il7r, Klrg1), whereas CD127-ST2- ILCs highly expressed ILC1-specific genes (Gzma, Gzmb, Irf8, Klrk1, and Klrb1) (**Figure 5**). Further, gene ontology analysis indicated that one of the most differentially expressed pathways between CD127+ST2+ and CD127-ST2- ILCs was IFNγ production (**Figure 6**). Thus, CD127+ST2+ and CD127-ST2- populations exhibit strong ILC2 and ILC1 signatures, respectively.

Intranasal CDG challenge strikingly reduced the total number of *Alt*-induced IL-5+ and IL-13+ CD127+ST2+ pulmonary ILCs post *ex vivo* PMA/ionomycin stimulation (**Figure 7A**). Red5 IL-5 reporters and Smart13 IL-13 reporters were utilized to provide *in vivo* evidence of CDG-induced ILC2 suppression [17, 18]. Unsurprisingly, similar trends between *ex vivo* and *in vivo* were demonstrated following Alt plus CDG treatment of reporter mice; CDG abrogated Alt-induced IL-5 and IL-13 production by ILC2s (**Figure 8**).

Contrary to ILC2 effector cytokines, the total number of IFNγ+ ILC1s significantly increased post CDG challenge and *ex vivo* PMA/ionomycin stimulation (**Figure 7B**). Conventional NK cells are also known to contribute to IFNγ levels, therefore we aimed to assess both numbers and activity of pulmonary NK cells. Interestingly, there was an observable increase in NK1.1+CD49b+CD3- lymphocytes in *Alt,* CDG, and *Alt* plus CDG exposed murine lungs relative to PBS (**Figure 14A**). However, there was no significant difference in NK cell IFNγ levels between each treatment group (**Figure 14B**), suggesting that IFNγ are not differentially responsive to *Alt*

plus CDG exposure, nor are contributing to overall IFNγ burden, as compared to CD127-ST2- ILCs.

Considering data demonstrating CDG-driven shift from ILC2 to ILC1 plasticity [22, 23], we aimed to further investigate the impact of CDG on ILC identity, activation, and proliferation. CDG induced suppression of pulmonary ILC2 master type 2 cytokine regulator GATA3 (**Figure 9**) while promoting increases in ILC1 expression of master type 1 cytokine regulator T-bet (**Figure 9**). Regarding proliferation and activation, CDG suppressed ILC2 proliferation demonstrated by a decrease in Ki67 expression (**Figure 12**) but no observable effects on ILC2 activation demonstrated by no change in CD69 (**Figure 13**). Conversely, CDG had no impact on ILC1 proliferation (Figure 12), yet significantly increased ILC1 activation status (**Figure 13**). Collectively, these findings suggest that CDG drivers associated ILC2 suppression and ILC1 activation.

CDG-driven suppression of type 2 inflammation is STING-dependent

With the observed strong airway IFN levels induced by CDG treatment, we aimed to determine whether STING was necessary for the suppression of type 2 inflammation and ILC2 responses. Surprisingly, STING deficient (*Tmem173-/-*) mice exhibited restored eosinophilia and fully abolished CDG-driven neutrophilia in the lung (**Figure 10**), a similar response to WT mice treated with *Alt* only.

CDG-induced suppression of type 2 inflammation requires Type 1 IFN signaling

Type 1 IFNs are considered major products of STING activation. To assess whether type 1 IFN production played a significant role in the observed CDG-induced immunomodulation, we

utilized type 1 IFN receptor deficient (*Ifnar1-/-*) mice in comparison to WT and *Tmem173-/-* mice. *Ifnar1-/-* restored CDG-induced reduction of BAL and lung eosinophilia but had no effect on BAL and lung neutrophilia (**Figure 11A, B**). Thus, type 1 IFNs are necessary for CDG-mediated suppression of type.2 inflammation but not for neutrophilia. Overall, these results are consistent with recent studies demonstrating the suppressive role type 1 IFNs have on pulmonary ILC2s during viral infection [20].

DISCUSSION

Conventionally classified by type 2 pulmonary inflammation, asthma is also associated with co-occurrent viral and bacterial infections, mitochondrial stress, and host cell death, collectively driving the buildup of danger-associated signaling cyclic-di-nucleotides [24-28]. Group 2 ILCs promote type 2 inflammation in murine models and likely contribute to AHR and airway inflammation in humans (29). Our work investigated how *in vivo* exposure of CDG regulated ILC2 and innate type 2 inflammation in the context of asthma. Our novel findings demonstrate that intranasal exposure to CDG nearly eradicated *Alt*-induced airway eosinophilia and promoted neutrophilia. Additionally, CDG drove suppression of ILC2 IL-5 and IL-13 production and increases in ILC1 IFNγ production. Mechanistically, we discovered that CDG modulated ILC activity downstream of *Alt*-induced inflammation, which was entirely dependent on STING-cGAS and type 1 IFN signaling. Therefore, STING's role in pathogenic responses, including activating by cytosolic mitochondrial DNA (from mitochondrial damage) and autophagy, could reflect a critical yet common relationship in the development of mixed airway inflammation [30-35].

Though STING-cGAS activity elicits major downstream production of type 1 IFNs, STING agonism has also demonstrated induction of several inflammatory mediators including CCL2, CCL20, IL1ß, IL-6, TNFα, and type 3 IFNs [36-39]. While type 1 IFNs exhibited increases post *Alt* plus CDG treatment, type 3 IFN (lambda) also showed increases but failed to demonstrated significance. Additionally, while types 1-3 IFNs have been shown to inhibit ILC2 responses and type 2 inflammation [19-21, 40-41], type 1 IFNs alone were required for CDG-driven ILC2 suppression. Collectively, our findings suggest a novel model in which intranasal CDG treatment promotes early STING-dependent production of type 1 IFN by respiratory phagocytes, thereby

inhibiting ILC2-driven airway eosinophilia. Additionally, the impact CDG effects on *Alt*-induced neutrophilia was independent of type 1 IFN signaling, suggesting that non-IFN inflammatory mediators downstream of STING activation may contribute to CDG-induced neutrophil trafficking.

STING effects on ILC activity and lung inflammation reported here demonstrate novelty, especially in tissue specific immunity. A recent study elucidating the role of STING in a gastrointestinal context reported an approximate 2-fold reduction in ILC2 frequency, IL-4 and IL-13 levels, and a 3-fold increase in ILC1 frequency in STING deficient mice within the mucosa [42]. Alternatively, we reported notable increases in respiratory ILCs and type 2 cytokines with decreased ILC1s and type 1 cytokines of *Tmem173-/-* mice post *Alt* plus CDG treatment. Our results are consistent with a study demonstrating ILC responses in other tissue types. Such converse findings suggest the role of tissue-specific mechanisms by way of STING influences on ILC responses [43].

Our study presents limitations in mechanisms downstream of STING that may drive airway neutrophilia to remain to be seen. In summary, our data demonstrates that CDG drives IFN production in a STING-dependent manner, thereby increasing ILC1 activation while suppressing innate type 2 inflammation.

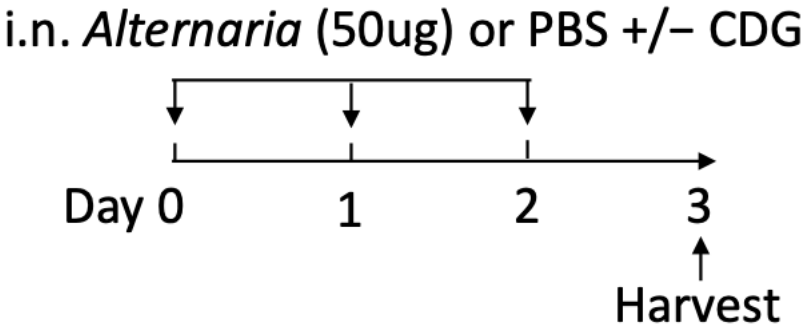

Figure 1. WT, *Tmem173-/-*, and *Ifnar1-/-* mice were challenged via a 3-day protocol. Mice were challenged with PBS, 50μg *Alternaria*, 5μg CDG, or 50μg *Alternaria* plus 5μg CDG on D0, D1, and D2. Mice were sacked on D3 and lungs and BAL were collected.

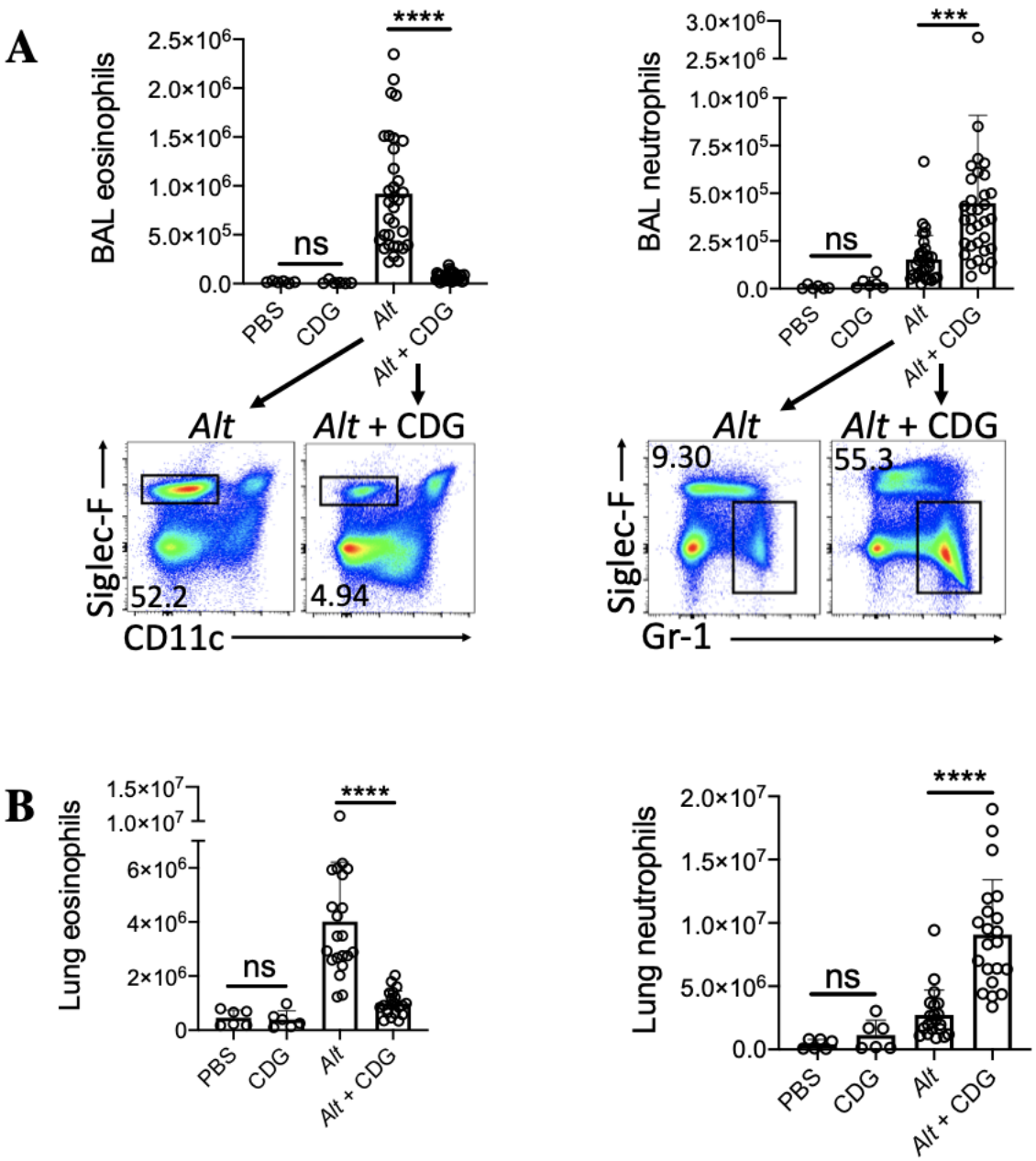

Figure 2. CDG attenuates BAL and lung eosinophilia in an *Alternaria* model. Mice were challenged using the model outlined in **Figure 1**. (A) Total BAL eosinophils and neutrophils with representative flow cytometric plots. (B) Total lung eosinophils and neutrophils. Data shown are representative of 2–10 independent experiments with 2–4 mice per group. $^{**}P < 0.01$, $^{***}P < 0.001$, $^{****}P < 0.0001$, unpaired *t*-test.

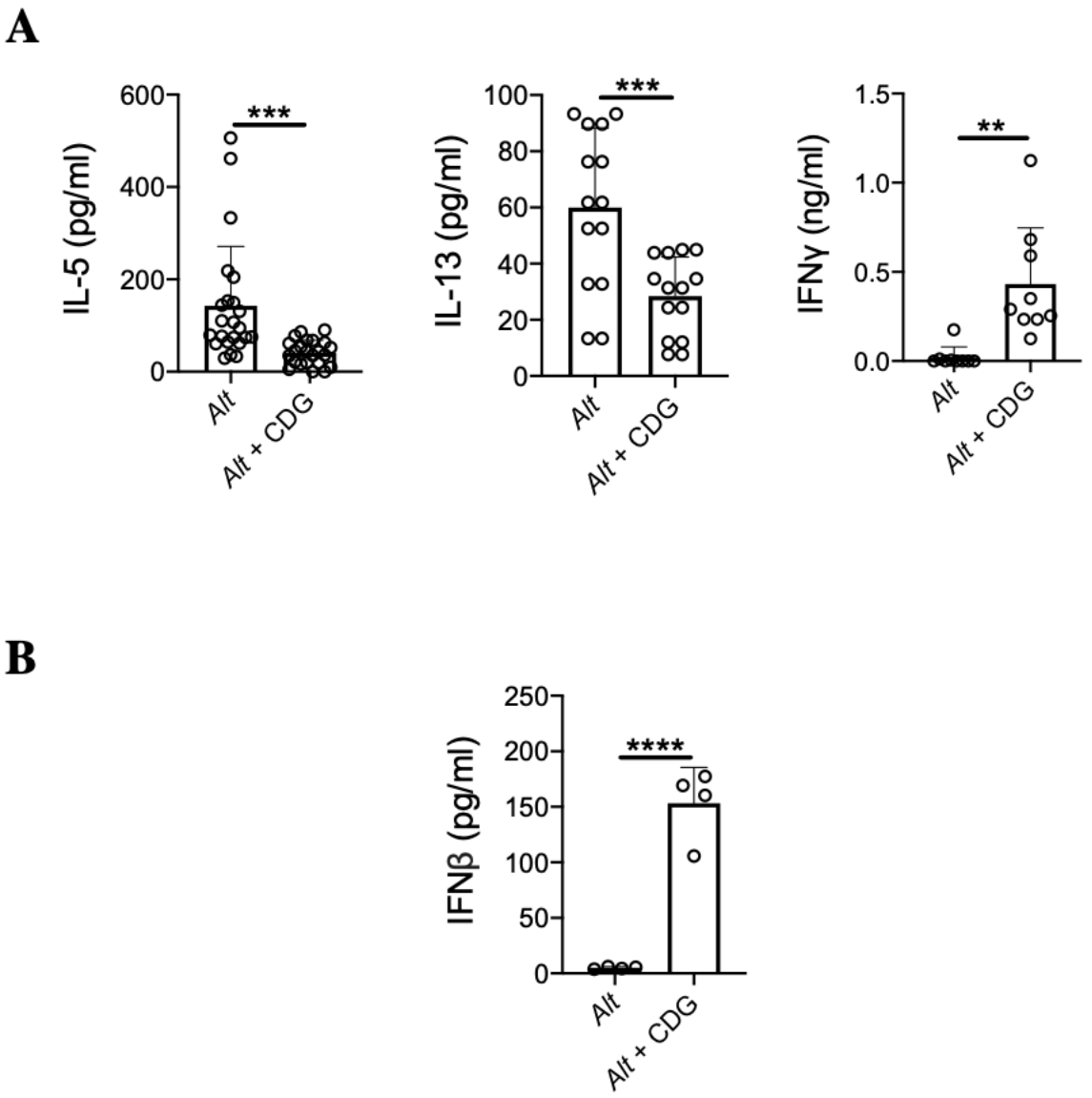

Figure 3. CDG attenuates BAL type 2 cytokines while promoting type 1 cytokines in an *Alternaria* model. Mice were challenged using the model outlined in **Figure 1**. (A) BAL ELISA of type 2 cytokines IL-5 and IL-13 and type 1 cytokine IFNγ. (B) BAL IFNß ELISA 3-hr post-intranasal challenge. Data shown are representative of 2–10 independent experiments with 2–4 mice per group. $^{**}P < 0.01$, $^{***}P < 0.001$, $^{****}P < 0.0001$, unpaired *t*-test.

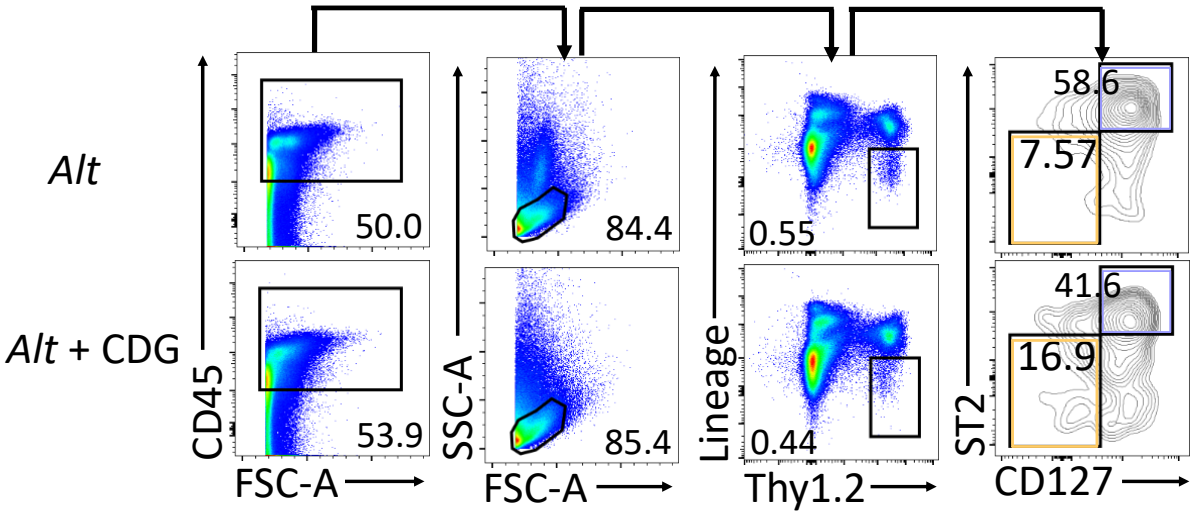

Figure 4. Flow cytometric gating scheme to identify pulmonary ILC2s and ILC1s post-intranasal treatment. Mice were challenged using the model outlined in **Figure 1**.

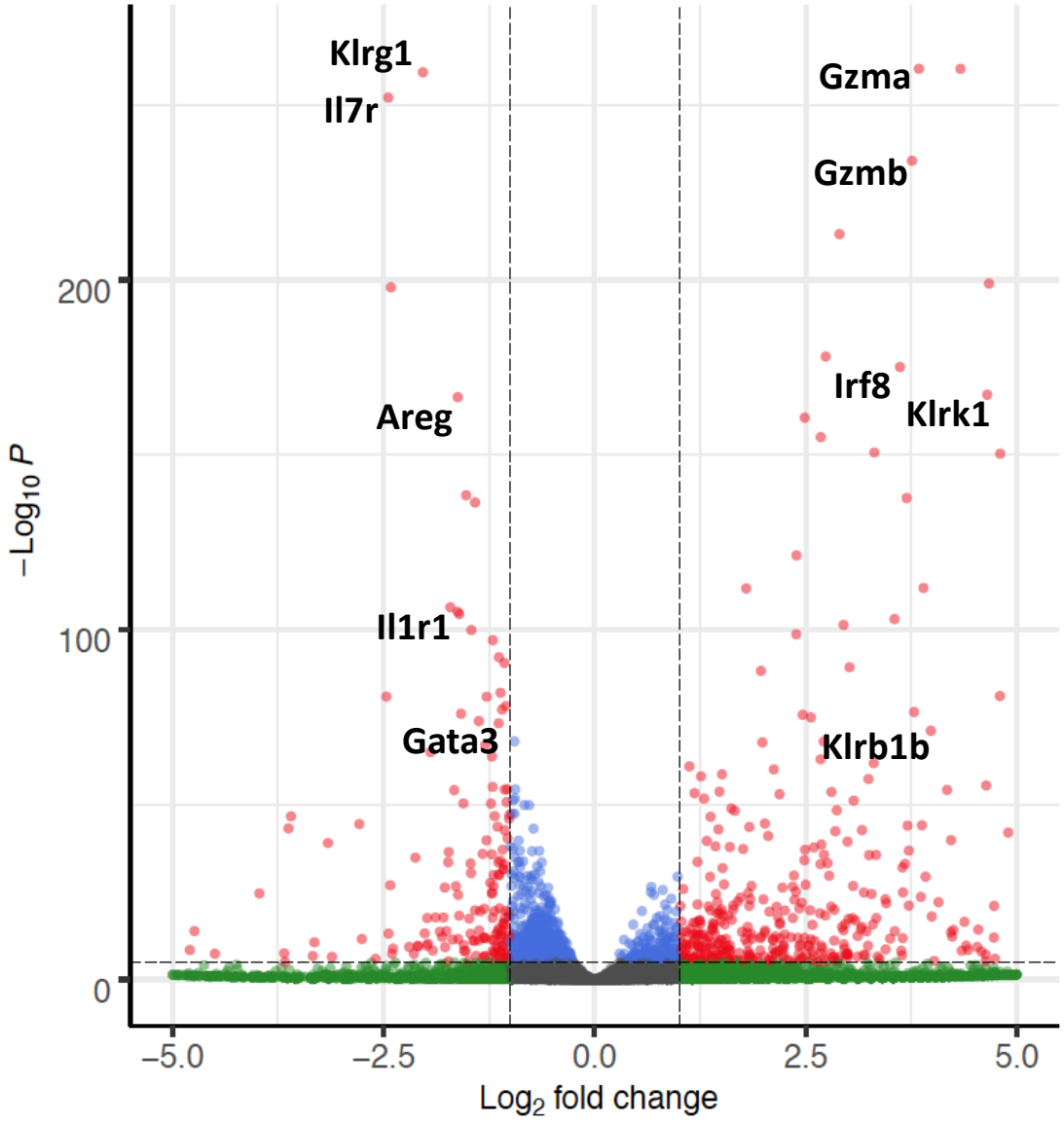

Figure 5. RNAseq volcano plot of differentially expressed genes of ST2+CD127+ versus ST2-CD127- pulmonary ILCs post-Alt challenge. Data shown are representative of 2–7 independent experiments with 2–4 mice per group.

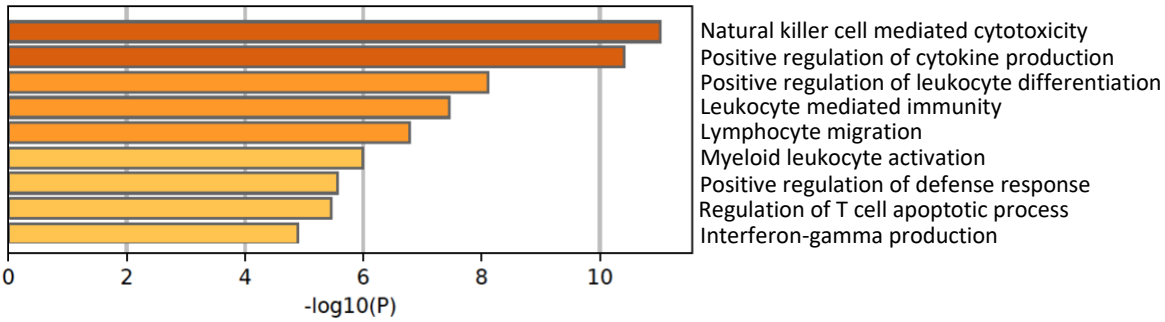

Figure 6. Differentially expressed gene ontologies in ST2+CD127+ and ST2-CD127- ILCs. Data shown are representative of 2–7 independent experiments with 2–4 mice per group.

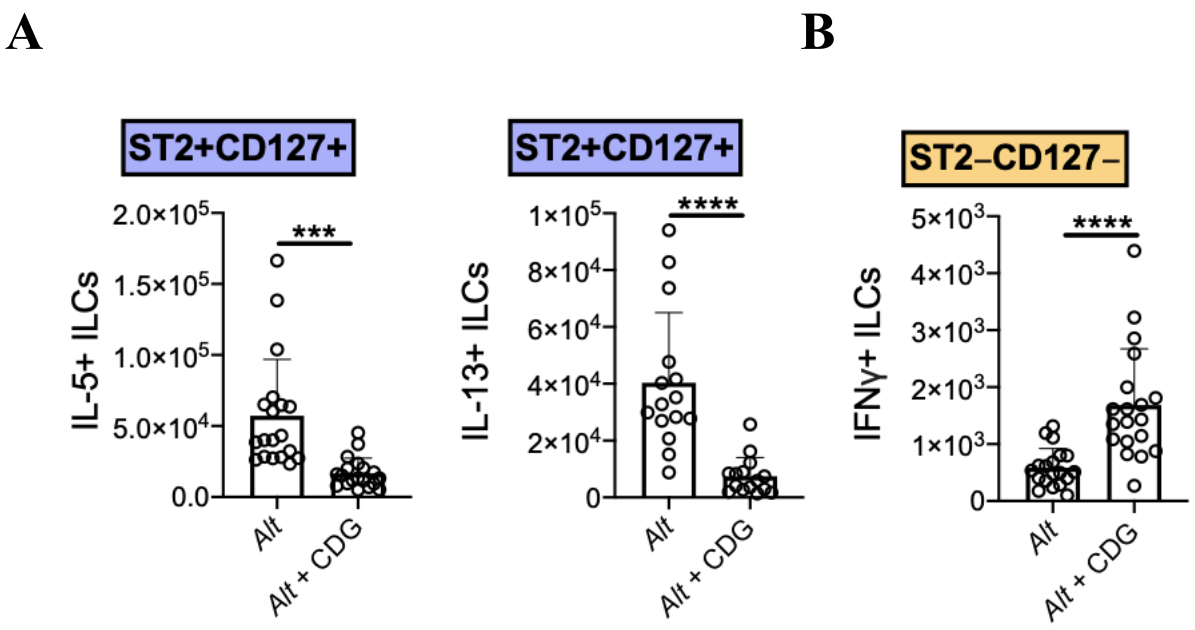

Figure 7. Total number of IL5+ and IL13+ ILC2s and IFNγ+ ILC1s after 3-hr PMA /ionomycin stimulation ex vivo. Mice were challenged using the model outlined in **Figure 1**. (**A**) Total IL-5 and IL-13 ST2+CD127+ pulmonary ILCs. (**B**) Total IFNγ ST2-CD127- pulmonary ILCs. Data shown are representative of 2–7 independent experiments with 2–4 mice per group. $^{*}P < 0.05$, $^{**}P < 0.01$, $^{***}P < 0.001$, $^{****}P < 0.0001$, unpaired t-test.

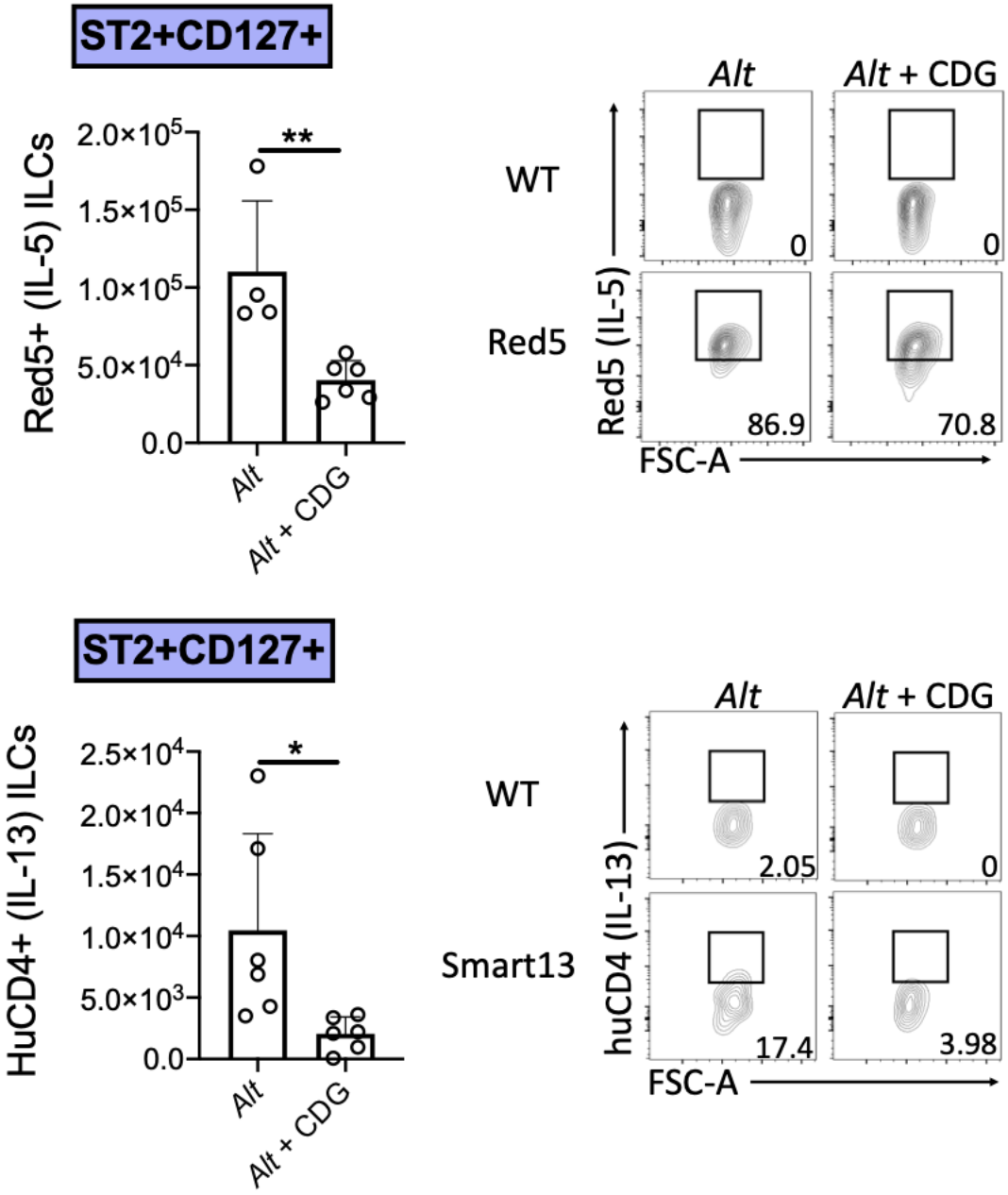

Figure 8. Total red-5+ (IL-5+) (top) and Smart13+ (IL-13+) (bottom) ST2+CD127+ ILCs with representative flow plots (right). Mice were challenged using the model outlined in **Figure 1**. Data shown are representative of 2–7 independent experiments with 2–4 mice per group. $^{*}P < 0.05$, $^{**}P < 0.01$, $^{***}P < 0.001$, $^{****}P < 0.0001$, unpaired t-test.

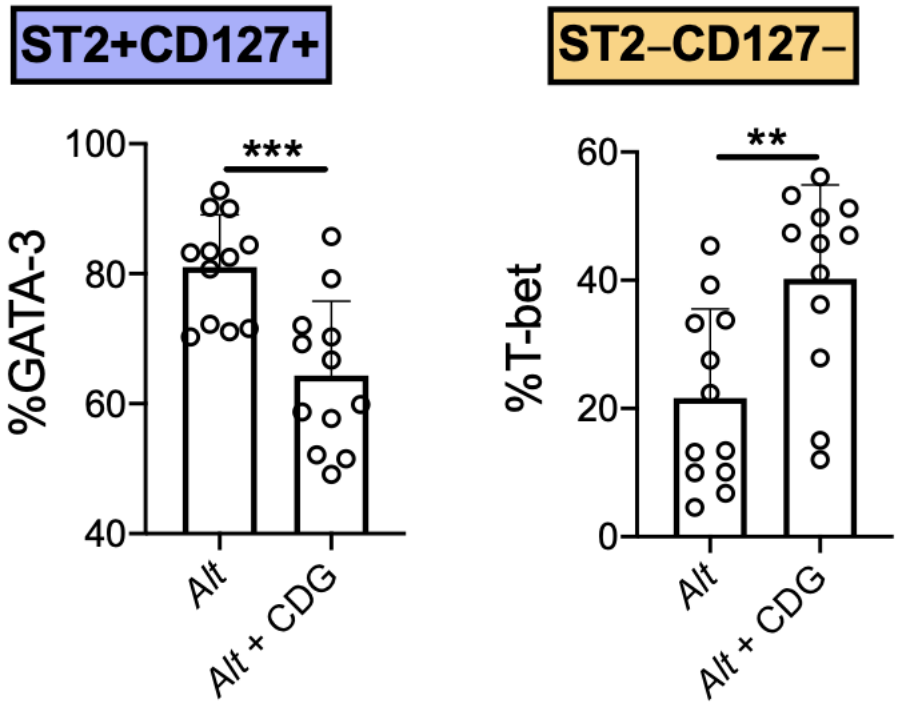

Figure 9. Frequency of GATA3+ ILC2s and T-bet+ ILC1s. Mice were challenged using the model outlined in **Figure 1**. Data shown are representative of 2–7 independent experiments with 2–4 mice per group. $^{*}P < 0.05$, $^{**}P < 0.01$, $^{***}P < 0.001$, $^{****}P < 0.0001$, unpaired t-test.

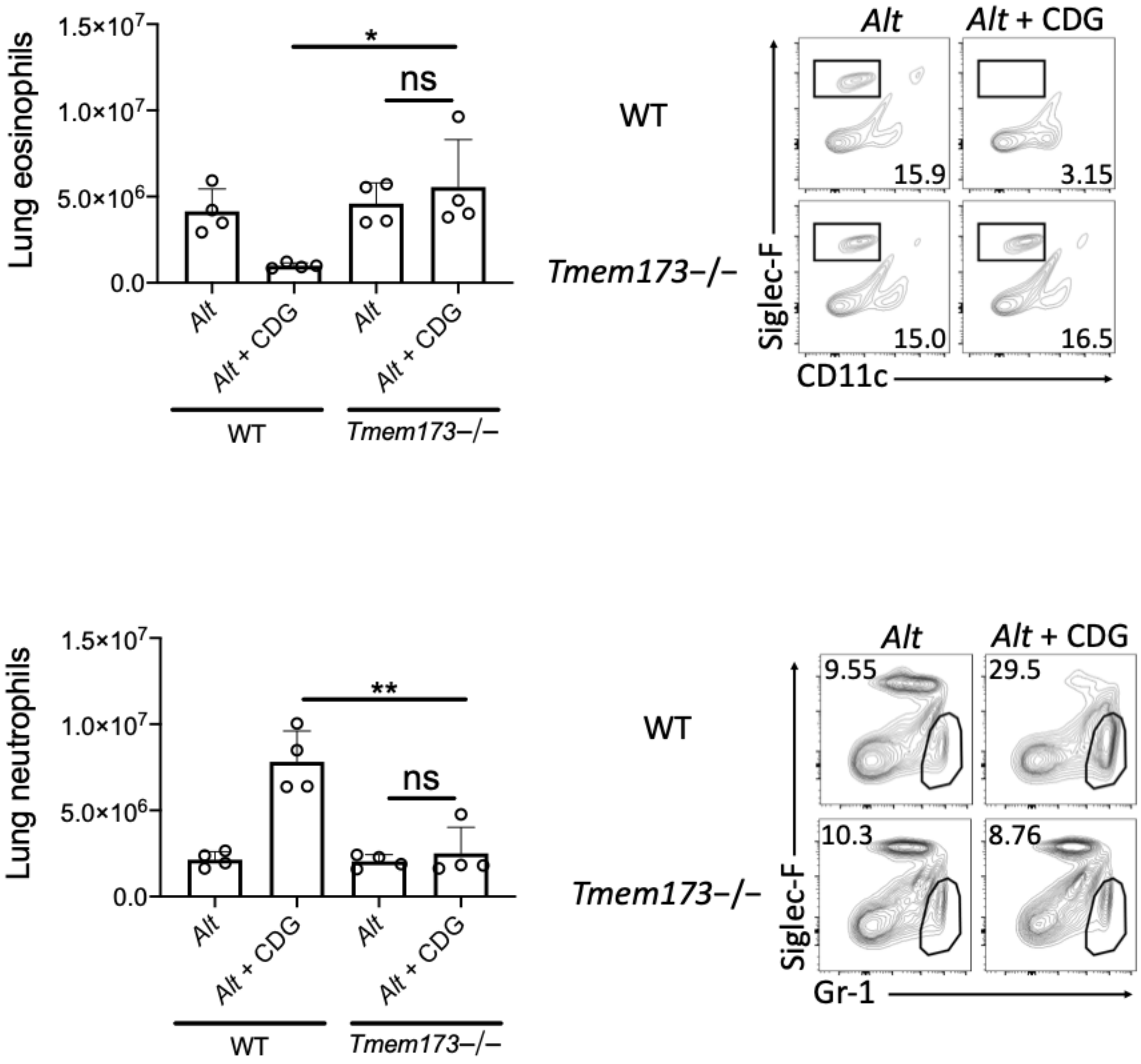

Figure 10. CDG modulation of pulmonary inflammation is STING-dependent. Mice were challenged using the model outlined in **Figure 1**. Total lung eosinophils (top) and neutrophils (bottom) with representative flow plots (right). Data shown are representative of 2–7 independent experiments with 2–4 mice per group. $^{*}P < 0.05$, $^{**}P < 0.01$, $^{****}P < 0.0001$, unpaired *t*-test.

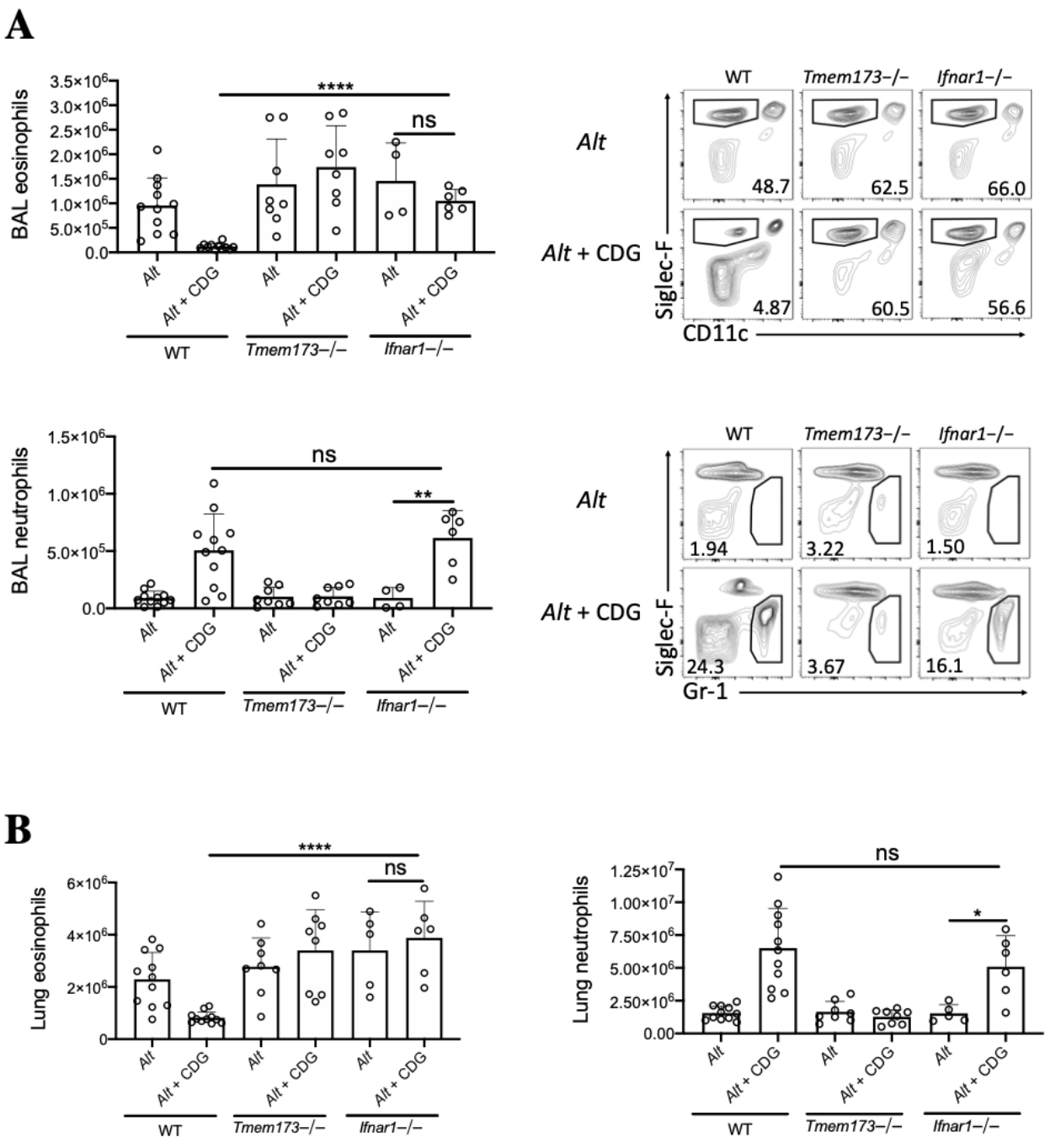

Figure 11. Type 1 IFN signaling is necessary for CDG driven suppression of airway and pulmonary type 2 inflammation. Mice were challenged using the model outlined in **Figure 1**. **(A)** Total BAL eosinophils (top) and neutrophils (bottom) with representative flow plots (right). **(B)** Total pulmonary eosinophils (top) and neutrophils (bottom) with representative flow plots (right). $^{*}P < 0.05$, $^{**}P < 0.01$, $^{***}P < 0.001$, $^{****}P < 0.0001$, unpaired t-test.

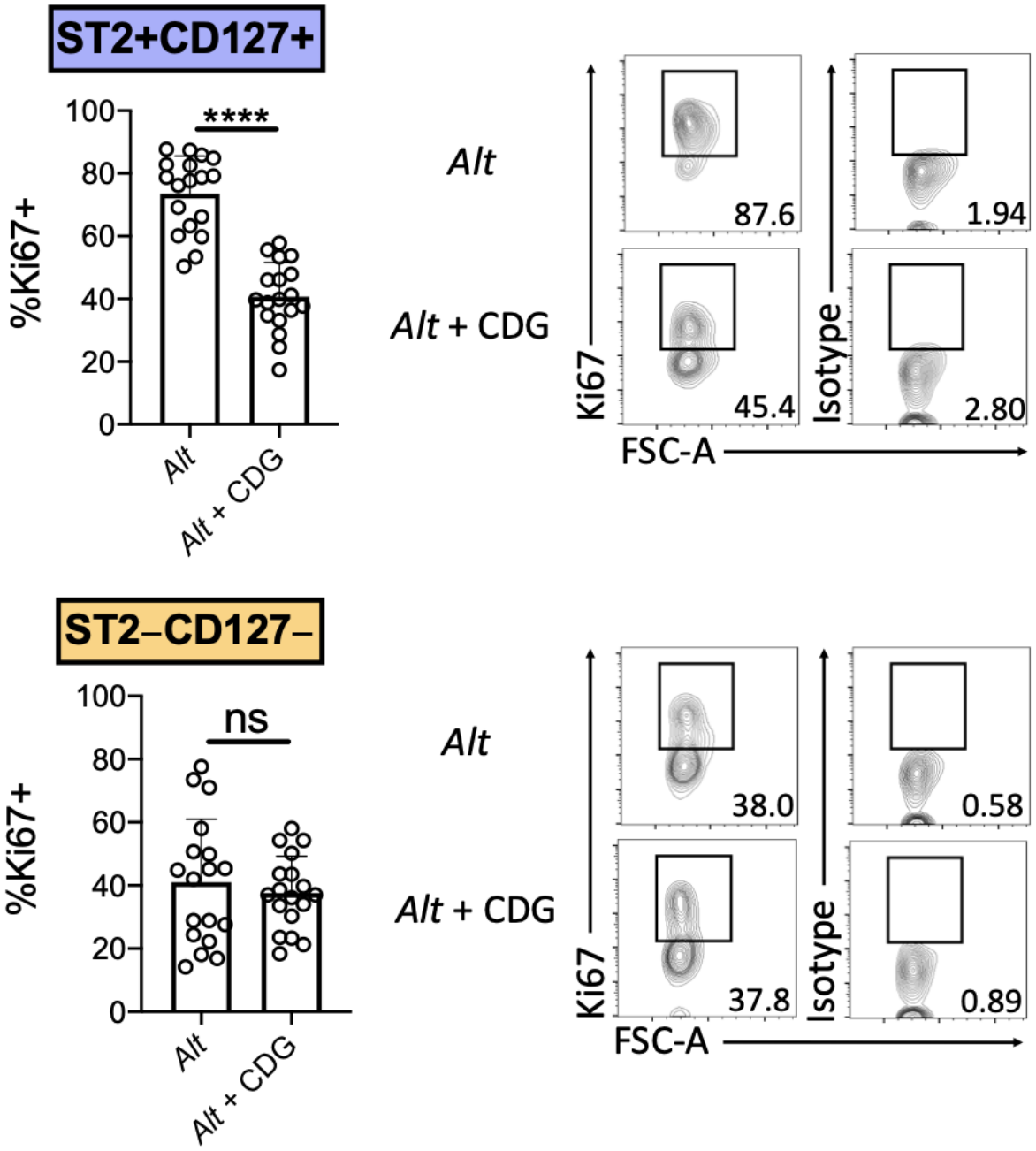

Figure 12. CDG suppresses proliferation in ST2+CD127+ ILCs. Mice were challenged using the model outlined in **Figure 1**. Ki67 expression in ST2+CD127+ ILCs (top) and ST2-CD127- ILCs (bottom) and representative flow plots (right). Mice were challenged using the model outlined in **Figure 1**. Data shown are representative of 2-7 independent experiments with 2-4 mice per group. $^{**}P < .01$, $^{***}P < .001$, $^{****}P < .0001$ unpaired t test.

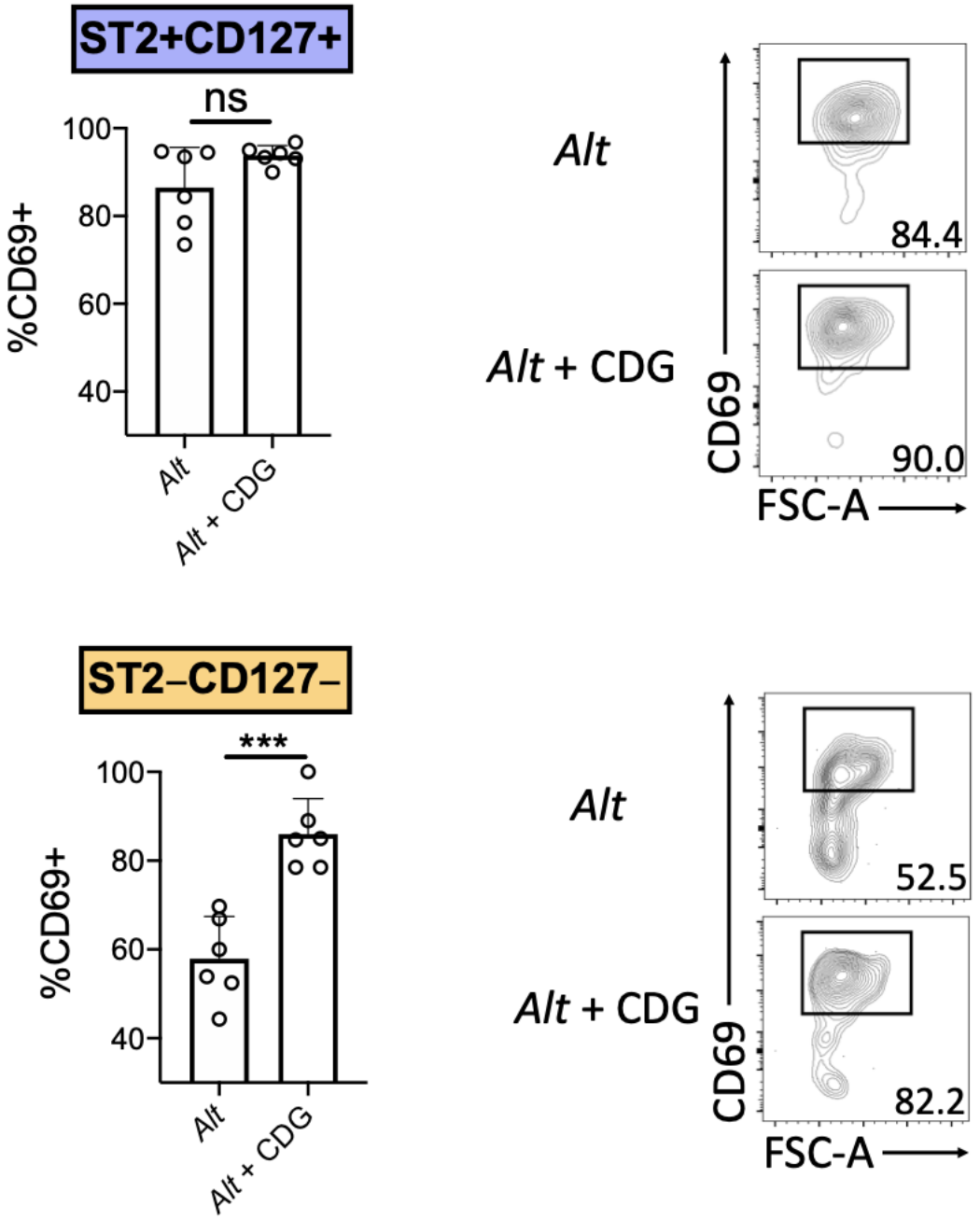

Figure 13. CDG promotes CD69 expression of ST2-CD127- ILCs. Mice were challenged using the model outlined in **Figure 1**. CD69 expression in ST2+CD127+ ILCs (top) and ST2-CD127- ILCs (bottom) and representative flow plots (right). Data shown are representative of 2-7 independent experiments with 2-4 mice per group. $^{**}P < .01$, $^{***}P < .001$, $^{****}P < .0001$ unpaired t test.

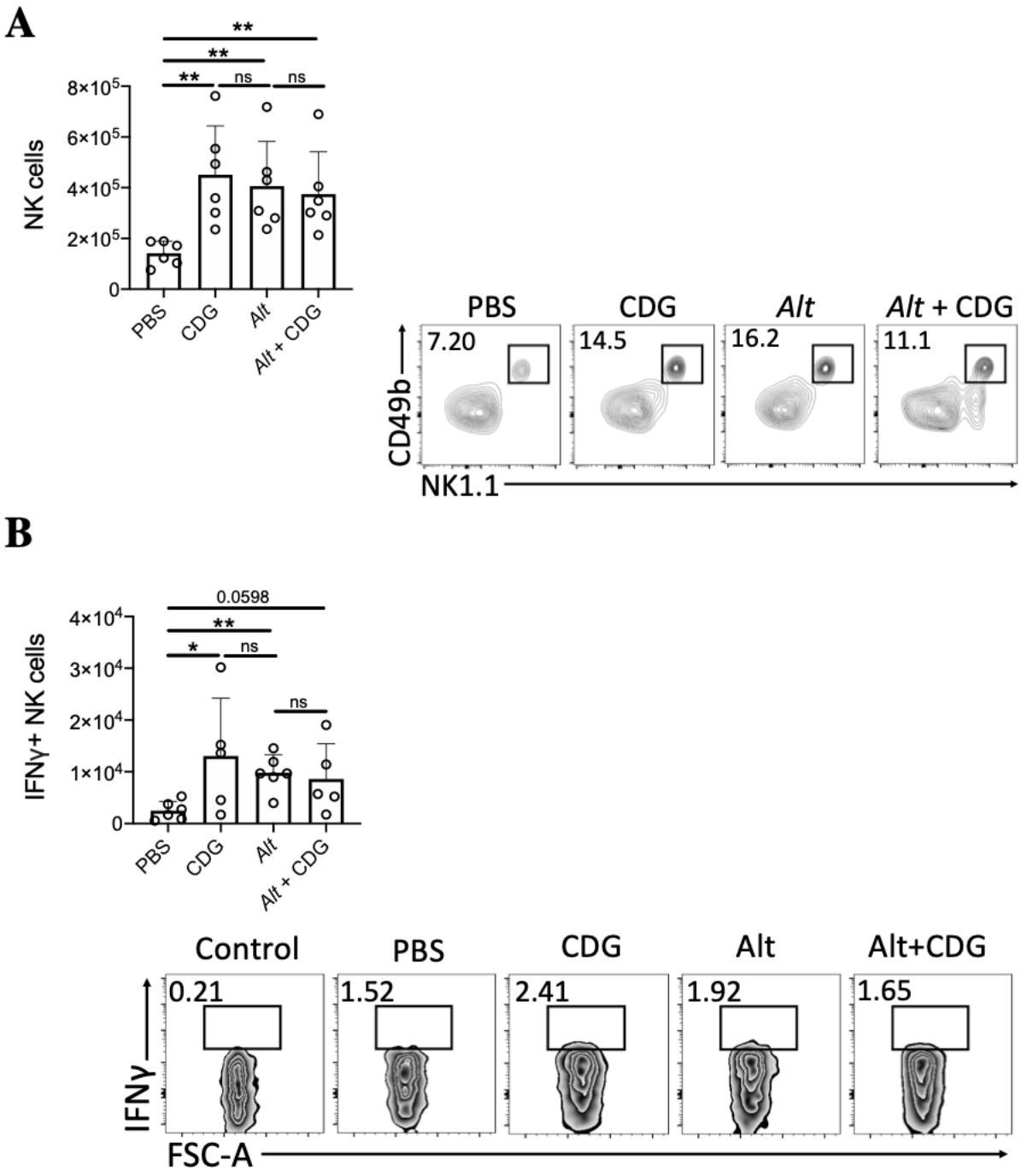

Figure 14. CDG does not potentiate Alt driven NK cell activation. Mice were challenged using the model outlined in **Figure 1**. **(A)** Total pulmonary NK cells (left) and representative flow plots (right). **(B)** Total IFNγ+ pulmonary NK cells (left) and representative flow plots (right). Data shown are representative of 2 independent experiments with 2-3 mice per group. $^{*}P < .05$, $^{**}P < .01$, unpaired t test.

The content of this thesis is a reprint of the material as it appears in Cyclic-di-GMP Induces STING-Dependent ILC2 to ILC1 Shift During Innate Type 2 Lung Inflammation 2021. Cavagnero, Kellen; Badrani, Jana; Naji, Luay; Amadeo, Michael; Leng, Anthea; Lacasa, Lee Diego; Strohm, Allyssa; Renusch, Samantha; Gasparian, Suzanna; Doherty, Taylor, Frontiers Media S.A., 2021. The thesis author was a co-author of this paper.

REFERENCES

1. Papi, A., Brightling, C., Pedersen, S.E., Reddel, H.K., 2018. Asthma. The Lancet 391, 783–800. https://doi.org/10.1016/S0140-6736(17)33311-1

2. Subbarao, P., Mandhane, P.J., Sears, M.R., 2009. Asthma: epidemiology, etiology and risk factors. Canadian Medical Association Journal 181, E181–E190. https://doi.org/10.1503/cmaj.080612

3. Kudo, M., Ishigatsubo, Y., Aoki, I., 2013. Pathology of asthma. Front. Microbiol. 4. https://doi.org/10.3389/fmicb.2013.00263

4. Holgate, S.T., 2008. Pathogenesis of Asthma. Clin Exp Allergy 38, 872–897. https://doi.org/10.1111/j.1365-2222.2008.02971.x

5. Aristizábal, B., González, Á. "Innate Immune System." *Autoimmunity: From Bench to Bedside [Internet]*., U.S. National Library of Medicine, 18 July 2013, https://www.ncbi.nlm.nih.gov/books/NBK459455/.

6. Spits, H., Artis, D., Colonna, M., Diefenbach, A., Di Santo, J.P., Eberl, G., Koyasu, S., Locksley, R.M., McKenzie, A.N.J., Mebius, R.E., Powrie, F., Vivier, E., 2013. Innate lymphoid cells — a proposal for uniform nomenclature. Nat Rev Immunol 13, 145–149. https://doi.org/10.1038/nri3365

7. Harly, C., Cam, M., Kaye, J., Bhandoola, A., 2018. Development and differentiation of early innate lymphoid progenitors. Journal of Experimental Medicine 215, 249–262. https://doi.org/10.1084/jem.20170832

8. Klose, C.S.N., Artis, D., 2016. Innate lymphoid cells as regulators of immunity, inflammation and tissue homeostasis. Nat Immunol 17, 765–774. https://doi.org/10.1038/ni.3489

9. An, Z., Flores-Borja, F., Irshad, S., Deng, J., Ng, T., 2020. Pleiotropic Role and Bidirectional Immunomodulation of Innate Lymphoid Cells in Cancer. Front. Immunol. 10, 3111. https://doi.org/10.3389/fimmu.2019.03111

10. Helfrich, S., Mindt, B.C., Fritz, J.H., Duerr, C.U., 2019. Group 2 Innate Lymphoid Cells in Respiratory Allergic Inflammation. Front. Immunol. 10, 930. https://doi.org/10.3389/fimmu.2019.00930

11. Duerr, C.U., Fritz, J.H., 2016. Regulation of group 2 innate lymphoid cells. Cytokine 87, 1–8. https://doi.org/10.1016/j.cyto.2016.01.018

12. Wan, D., Jiang, W., Hao, J., 2020. Research Advances in How the cGAS-STING Pathway Controls the Cellular Inflammatory Response. Front. Immunol. 11, 615. https://doi.org/10.3389/fimmu.2020.00615

13. Woodward, J.J., Iavarone, A.T., Portnoy, D.A., 2010. c-di-AMP Secreted by Intracellular *Listeria monocytogenes* Activates a Host Type I Interferon Response. Science 328, 1703–1705. https://doi.org/10.1126/science.1189801

14. Burdette, D.L., Monroe, K.M., Sotelo-Troha, K., Iwig, J.S., Eckert, B., Hyodo, M., Hayakawa, Y., Vance, R.E., 2011. STING is a direct innate immune sensor of cyclic di-GMP. Nature 478, 515–518. https://doi.org/10.1038/nature10429

15. Raundhal, M., Morse, C., Khare, A., Oriss, T.B., Milosevic, J., Trudeau, J., Huff, R., Pilewski, J., Holguin, F., Kolls, J., Wenzel, S., Ray, P., Ray, A., 2015. High IFN-γ and low SLPI mark severe asthma in mice and humans. J. Clin. Invest. 125, 3037–3050. https://doi.org/10.1172/JCI80911

16. Cavagnero, K.J., Badrani, J.H., Naji, L.H., Amadeo, M.B., Shah, V.S., Gasparian, S., Pham, A., Wang, A.W., Seumois, G., Croft, M., Broide, D.H., Doherty, T.A., 2019. Unconventional ST2- and CD127-negative lung ILC2 populations are induced by the fungal allergen Alternaria alternata. Journal of Allergy and Clinical Immunology 144, 1432-1435.e9. https://doi.org/10.1016/j.jaci.2019.07.018

17. Nussbaum, J.C., Van Dyken, S.J., von Moltke, J., Cheng, L.E., Mohapatra, A., Molofsky, A.B., Thornton, E.E., Krummel, M.F., Chawla, A., Liang, H.-E., Locksley, R.M., 2013. Type 2 innate lymphoid cells control eosinophil homeostasis. Nature 502, 245–248. https://doi.org/10.1038/nature12526

18. Liang, H.-E., Reinhardt, R.L., Bando, J.K., Sullivan, B.M., Ho, I.-C., Locksley, R.M., 2012. Divergent expression patterns of IL-4 and IL-13 define unique functions in allergic immunity. Nat Immunol 13, 58–66. https://doi.org/10.1038/ni.2182

19. Molofsky, A.B., Van Gool, F., Liang, H.-E., Van Dyken, S.J., Nussbaum, J.C., Lee, J., Bluestone, J.A., Locksley, R.M., 2015. Interleukin-33 and Interferon-γ Counter-Regulate Group 2 Innate Lymphoid Cell Activation during Immune Perturbation. Immunity 43, 161–174. https://doi.org/10.1016/j.immuni.2015.05.019

20. Duerr, C.U., McCarthy, C.D.A., Mindt, B.C., Rubio, M., Meli, A.P., Pothlichet, J., Eva, M.M., Gauchat, J.-F., Qureshi, S.T., Mazer, B.D., Mossman, K.L., Malo, D., Gamero, A.M., Vidal, S.M., King, I.L., Sarfati, M., Fritz, J.H., 2016. Type I interferon restricts type 2 immunopathology through the regulation of group 2 innate lymphoid cells. Nat Immunol 17, 65–75. https://doi.org/10.1038/ni.3308

21. Califano, D., Furuya, Y., Roberts, S., Avram, D., McKenzie, A.N.J., Metzger, D.W., 2018. IFN-γ increases susceptibility to influenza A infection through suppression of group II innate lymphoid cells. Mucosal Immunol 11, 209–219. https://doi.org/10.1038/mi.2017.41

22. Krabbendam, L., Bal, S.M., Spits, H., Golebski, K., 2018. New insights into the function, development, and plasticity of type 2 innate lymphoid cells. Immunol Rev 286, 74–85. https://doi.org/10.1111/imr.12708

23. Ealey, K.N., Moro, K., Koyasu, S., 2017. Are ILC 2s Jekyll and Hyde in airway inflammation? Immunol Rev 278, 207–218. https://doi.org/10.1111/imr.12547

24. Zhang, Q., Illing, R., Hui, C.K., Downey, K., Carr, D., Stearn, M., Alshafi, K., Menzies-Gow, A., Zhong, N., Fan Chung, K., 2012. Bacteria in sputum of stable severe asthma and increased airway wall thickness. Respir Res 13, 35. https://doi.org/10.1186/1465-9921-13-35

25. Holtzman, M.J., 2012. Asthma as a chronic disease of the innate and adaptive immune systems responding to viruses and allergens. J. Clin. Invest. 122, 2741–2748. https://doi.org/10.1172/JCI60325

26. Lambrecht, B.N., Hammad, H., 2013. Death at the airway epithelium in asthma. Cell Res 23, 588–589. https://doi.org/10.1038/cr.2013.26

27. Chen, Q., Sun, L., Chen, Z.J., 2016. Regulation and function of the cGAS–STING pathway of cytosolic DNA sensing. Nat Immunol 17, 1142–1149. https://doi.org/10.1038/ni.3558

28. Ban, G.-Y., Pham, D.L., Trinh, T.H.K., Lee, S.-I., Suh, D.-H., Yang, E.-M., Ye, Y.-M., Shin, Y.S., Chwae, Y.-J., Park, H.-S., 2016. Autophagy mechanisms in sputum and peripheral blood cells of patients with severe asthma: a new therapeutic target. Clin Exp Allergy 46, 48–59. https://doi.org/10.1111/cea.12585

29. Cavagnero, K., Doherty, T.A., 2017. Cytokine and Lipid Mediator Regulation of Group 2 Innate Lymphoid Cells (ILC2s) in Human Allergic Airway Disease. J Cytokine Biol 02. https://doi.org/10.4172/2576-3881.1000116

30. Chen, Q., Sun, L., Chen, Z.J., 2016. Regulation and function of the cGAS–STING pathway of cytosolic DNA sensing. Nat Immunol 17, 1142–1149. https://doi.org/10.1038/ni.3558

31. Barber, Glen N. “STING: Infection, Inflammation and Cancer.” Nature Reviews Immunology, vol. 15, no. 12, Dec. 2015, pp. 760–70. *DOI.org (Crossref)*, https://doi.org/10.1038/nri3921

32. Ray, A., Raundhal, M., Oriss, T.B., Ray, P., Wenzel, S.E., 2016. Current concepts of severe asthma. Journal of Clinical Investigation 126, 2394–2403. https://doi.org/10.1172/JCI84144

33. Benmerzoug, S., Rose, S., Bounab, B., Gosset, D., Duneau, L., Chenuet, P., Mollet, L., Le Bert, M., Lambers, C., Geleff, S., Roth, M., Fauconnier, L., Sedda, D., Carvalho, C., Perche, O., Laurenceau, D., Ryffel, B., Apetoh, L., Kiziltunc, A., Uslu, H., Albez, F.S., Akgun, M., Togbe, D., Quesniaux, V.F.J., 2018. STING-dependent sensing of self-DNA drives silica-induced lung inflammation. Nat Comm 9, 5226. https://doi.org/10.1038/s41467-018-07425-1

34. Liu, D., Wu, H., Wang, C., Li, Y., Tian, H., Siraj, S., Sehgal, S.A., Wang, X., Wang, J., Shang, Y., Jiang, Z., Liu, L., Chen, Q., 2019. STING directly activates autophagy to tune the innate immune response. Cell Death Differ 26, 1735–1749. https://doi.org/10.1038/s41418-018-0251-z

35. Gui, X., Yang, H., Li, T., Tan, X., Shi, P., Li, M., Du, F., Chen, Z.J., 2019. Autophagy induction via STING trafficking is a primordial function of the cGAS pathway. Nature 567, 262–266. https://doi.org/10.1038/s41586-019-1006-9

36. Burdette, D.L., Vance, R.E., 2013. STING and the innate immune response to nucleic acids in the cytosol. Nat Immunol 14, 19–26. https://doi.org/10.1038/ni.2491

37. Abe, T., Barber, G.N., 2014. Cytosolic-DNA-Mediated, STING-Dependent Proinflammatory Gene Induction Necessitates Canonical NF- B Activation through TBK1. Journal of Virology 88, 5328–5341. https://doi.org/10.1128/JVI.00037-14

38. Kim, J.-A., Park, S.-K., Seo, S.-W., Lee, C.-H., Shin, O.S., 2017. STING Is Involved in Antiviral Immune Response against VZV Infection via the Induction of Type I and III IFN Pathways. Journal of Investigative Dermatology 137, 2101–2109. https://doi.org/10.1016/j.jid.2017.03.041

39. Dunphy, G., Flannery, S.M., Almine, J.F., Connolly, D.J., Paulus, C., Jønsson, K.L., Jakobsen, M.R., Nevels, M.M., Bowie, A.G., Unterholzner, L., 2018. Non-canonical Activation of the DNA Sensing Adaptor STING by ATM and IFI16 Mediates NF-κB Signaling after Nuclear DNA Damage. Molecular Cell 71, 745-760.e5. https://doi.org/10.1016/j.molcel.2018.07.034

40. Gimeno Brias, S., Marsden, M., Forbester, J., Clement, M., Brandt, C., Harcourt, K., Kane, L., Chapman, L., Clare, S., Humphreys, I.R., 2018. Interferon lambda is required for interferon gamma-expressing NK cell responses but does not afford antiviral protection during acute and persistent murine cytomegalovirus infection. PLoS ONE 13, e0197596. https://doi.org/10.1371/journal.pone.0197596

41. Lee, A.J., Ashkar, A.A., 2018. The Dual Nature of Type I and Type II Interferons. Front. Immunol. 9, 2061. https://doi.org/10.3389/fimu.2018.02061

42. Canesso, M.C.C., Lemos, L., Neves, T.C., Marim, F.M., Castro, T.B.R., Veloso, É., Queiroz, C.P., Ahn, J., Santiago, H.C., Martins, F.S., Alves-Silva, J., Ferreira, E., Cara, D.C., Vieira, A.T., Barber, G.N., Oliveira, S.C., Faria, A.M.C., 2018. The cytosolic sensor STING is required for intestinal homeostasis and control of inflammation. Mucosal Immunol 11, 820–834. https://doi.org/10.1038/mi.2017.88

43. Ricardo-Gonzalez, R.R., Van Dyken, S.J., Schneider, C., Lee, J., Nussbaum, J.C., Liang, H.-E., Vaka, D., Eckalbar, W.L., Molofsky, A.B., Erle, D.J., Locksley, R.M., 2018. Tissue signals imprint ILC2 identity with anticipatory function. Nat Immunol 19, 1093–1099. https://doi.org/10.1038/s41590-018-0201-4